Searching for hidden matter with milliQan

Emily Pottebaum
Iowa State University
egpott@iastate.edu
(Dated: September 30, 2021)

The milliQan experiment will search for particles with a fraction of the charge of an electron during Run 3 of the Large Hadron Collider (LHC). There are two components of the detector design: the bar detector and the slab detector. In order to increase the charge sensitivity of the slab detector, we have designed a summing amplifier that will allow us to double the number of photomultiplier tubes (PMTs) per slab without increasing the number of output signals. The development of the summing amplifier and plans for future work are described here.

I. INTRODUCTION

Everything in the universe that can currently be observed is described by the Standard Model (SM) of particle physics. Comprehensive as it may seem, the SM only accounts for 5% of the mass-energy in the universe. A much larger portion–more than one quarter–is made of dark matter (DM), which does not interact electromagnetically but does have observable gravitational effects [1].

A growing number of theoretical and experimental searches for DM are looking to the conjectured dark sector, a collection of particles beyond the SM that are neutral to electromagnetism as well as the strong and weak forces. Experimental interest lies predominantly in the case of the dark photon, the dark sector counterpart of the SM photon. Through the process of kinetic mixing, a dark photon could interact with an SM photon. This interaction would physically manifest as an effective electric charge that could be one thousand times smaller than that of the electron. This is called a millicharged particle (mCP) [2].

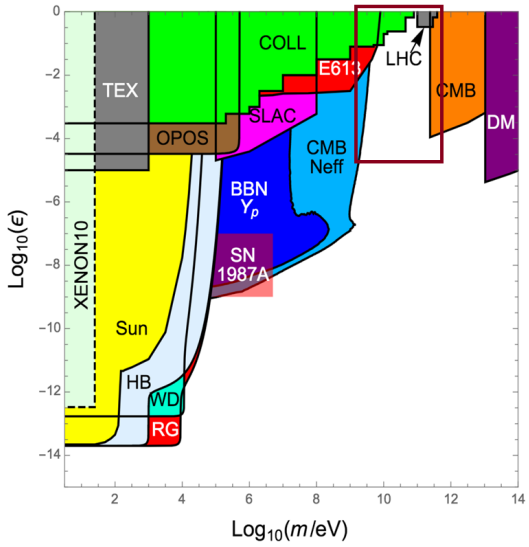

FIG. 1. mCP phase space, where ϵ is charge per eV and m is mass. milliQan will target the boxed region.

In the mass-charge parameter space of mCPs (see FIG. 1), the region of mass on the MeV-GeV border remains broadly unexplored at the time of writing [3]. The milliQan experiment will target this area.

II. DETECTOR

The milliQan detector includes both a bar and a slab detector. Pictured in FIG. 2, the bar detector consists of scintillator bars arranged into four layers. A PMT is connected to one end of each bar, and there are sixteen bars per layer. The bar detector is sensitive to particles with low mass and low charge. It will therefore be capable of detecting a high mCP flux limited by the low mass acceptance [4].

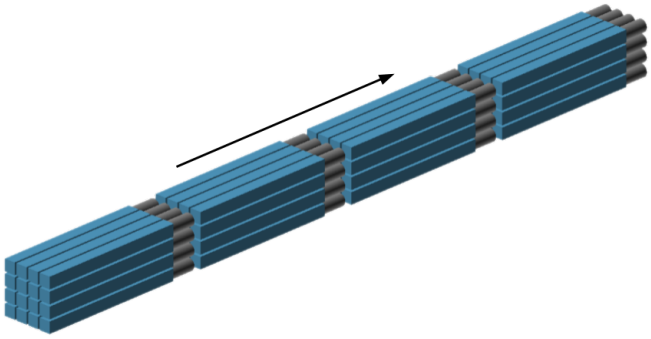

FIG. 2. A model of the milliQan bar detector. The arrow indicates the direction of particle travel.

The low mass limit of the bar detector inspired the design of a second detector with a higher mass acceptance. This is accomplished by utilizing scintillator slabs with a much greater surface area than that of the bars [4]. The slab detector design has four layers, with twelve slabs per layer and two PMTs per slab (see FIG. 3). This design is much more flexible than the bar detector, and the number of layers, slabs per layer, and PMTs per slab can easily be modified.

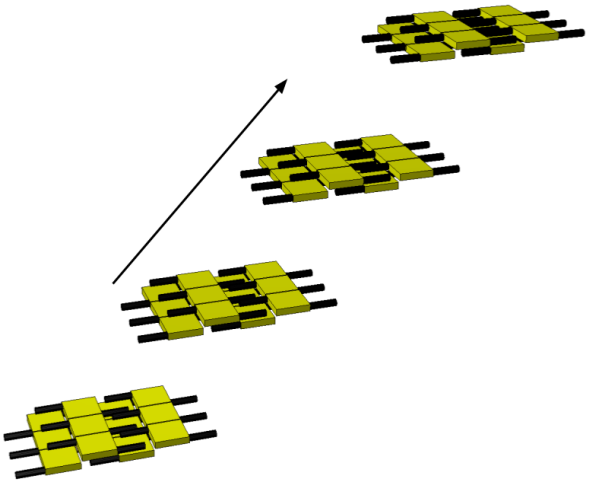

FIG. 3. Design for the milliQan slab detector [4]. The arrow indicates the direction of particle travel.

III. SUMMING AMPLIFIER

The improved mass coverage of the slab detector comes at the cost of charge sensitivity, but the design flexibility provides avenues to improve this. Increasing the number of PMTs per slab from two to four will increase the charge sensitivity, and the introduction of a summing amplifier will keep the number of output signals per slab at two.

A. Design

The printed circuit board (PCB), pictured in FIG. 4, was designed to be mounted along the edge of a scintillator slab between two PMTs. Signal from the PMTs is input by the SMA connectors located on either side of the board, and the output signal is sent via a third SMA connector. The board receives a +5V and -5V power supply through an 8 wire ribbon cable. A full schematic diagram of the summing amplifier can be found in Appendix A.

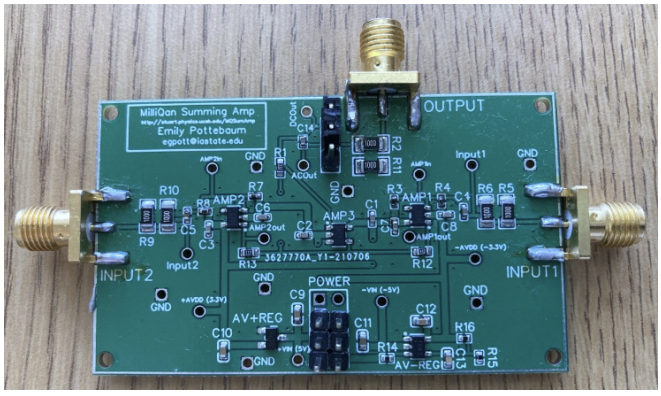

FIG. 4. The summing amplifier PCB.

B. Testing

Initial testing of the PCB was conducted remotely due to the COVID-19 pandemic. Instead of PMTs, the input signals were produced from cosmic rays detected by scintillator bars and Silicon photo-multipliers (SiPMs) [5].

The board received the signals via breadboard wires and was examined with the two-channel OpenScope MZ oscilloscope. Probing the board revealed noise being picked up by the breadboard wires and interfering with the cosmic ray signal.

To combat this issue, a direct connection between the cosmic ray readout board and the summing amplifier was established with an intermediate PCB that connected directly to the cosmic ray readout board and delivered signals to the summing amplifier via coaxial cables that are far better insulated from noise than breadboard wires. This setup used a four-channel oscilloscope, the DRS4 Evaluation Board, in order to examine both of the input signals and the output. Power was supplied to the connector and summing amplifier PCBs using a 5V PowerBRICK from Digilent. The modified testing setup is shown in FIG. 5.

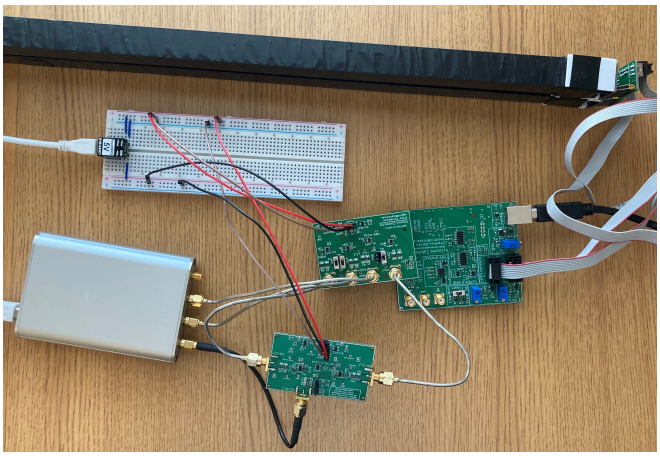

FIG. 5. Modified testing setup. From top to bottom: scintillator bars, power supply, cosmic ray readout and connector PCBs, DRS4 Evaluation Board, and summing amplifier PCB.

The output signal is expected to be the inverted sum of the two input signals. FIG. 6 shows that the output signal is inverted as expected. The DRS4 has an intrinsic impedance of 50Ω, and as the board is impedance matched the output signal is driven through an impedance of 100Ω, which sags the signal and is the reason the output amplitude for this testing setup is smaller than originally expected. The time lag between the input waveforms (see FIG. 6) is due to a time lag between operational amplifiers, and the ringing pattern present in the waveforms is due to signal reflections as the analog signals from the SiPMs are not well terminated. This ringing will not be present when using PMTs.

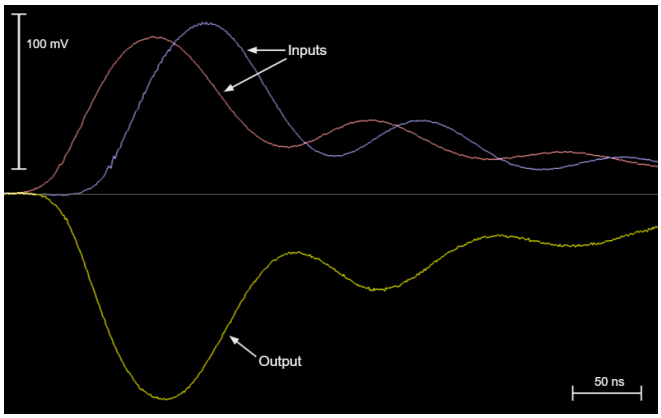

FIG. 6. Signal seen from the modified testing setup. The positive red and blue waveforms are the input cosmic ray signals, and the negative yellow waveform is the output signal.

C. Modifications

After the original PCB was tested, the design was modified accordingly. These updates included an additional unity gain buffer preceding the output signal, changing resistor values to obtain a positive DC offset, adding potentiometers to adjust that offset, and some superficial adjustments to the general layout. The modified board was sent to UCSB to be tested with PMT inputs.

Tests of the modified PCB with PMT inputs confirmed that the summing amplifier works and inspired a few more small modifications to make to the final design.

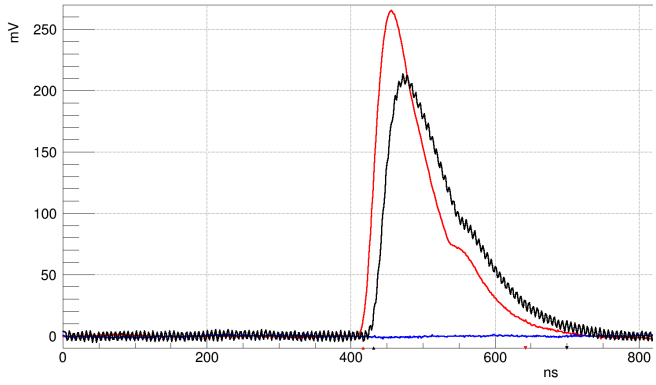

FIG. 7. Summing amp test using PMT inputs. The red line is signal from one PMT, and the black line is the output signal.

The black line in FIG. 7 shows oscillations in the output signal. Shielding the PCB with aluminum foil did not remove the oscillations, indicating they came from the board itself. The most likely cause was one or more of the unity gain buffer amplifiers (AMP1, AMP2, and AMP4 in Appendix A) responding to a resonant frequency. These amplifiers had a gain of two instead of one in the final design to avoid this issue. The final schematic can be found in Appendix A. The final PCB performed well on initial tests at UCSB (FIG. 8) and is now being sent to milliQan collaborators at New York University and the University of Nebraska to be tested with the slabs.

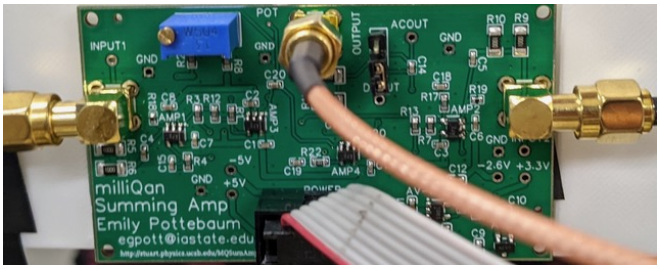

FIG. 8. Final PCB design.

D. PMT Characterization

Along with analyzing the output from the board, it was important to characterize signals from the PMTs in order to understand what the board was receiving as input. An incoming photon will produce a single photoelectron (SPE) inside the PMT (due to the photoelectric effect), which in turn will produce a large current of photoelectrons, which is converted to a voltage pulse after being output from the PMT. A histogram of voltage pulses for a given PMT can then be used to identify the SPE peak, which gives the characteristic output voltage for the PMT. An example output of the peak finding and fitting algorithm we have written is shown in FIG. 9. Beyond the testing and calibration of the summing amplifier, the characteristic SPE voltage for each PMT in the detector will need to be determined. This fitting algorithm will aid in the efficiency of this process.

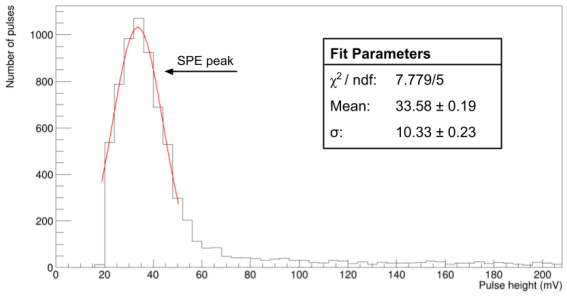

FIG. 9. A histogram of PMT output voltage pulses. The SPE peak has a Gaussian fit with parameters indicated in the figure.

IV. CONCLUSIONS AND FUTURE WORK

The final summing amplifier board works as expected, and the slab detector design has been updated to include four PMTs per slab instead of two. This means the milliQan slab detector will cover a broader region of the mCP charge-mass phase space, doubling the light sensitivity and therefore increasing the charge sensitivity by a factor of $\sqrt{2}$. FIG. 10 shows the projected detector sensitivity of the slab detector with two PMTs per slab [4]. With four PMTs per slab we expect the solid blue line to expand down to reach lower charges for mCPs of higher mass.

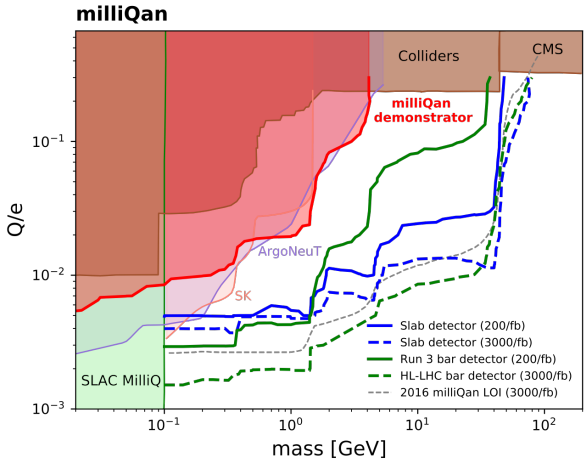

FIG. 10. milliQan detector sensitivity compared with that of other experiments. The slab detector is represented by the solid blue line. The dashed lines are the projected sensitivities for the upcoming high-luminosity LHC [4].

The immediate next step will be to test the summing amplifier with the slabs and ensure it works as expected with the intended setup. Going forward, the summing amplifier introduces extra calibration for the slab detector. The summed PMT signal should be understood and accounted for along with individual PMT calibration. We must also consider how four PMTs and two summing amplifier PCBs will be placed on each slab to optimize detection and readout efficiency. A mount for the PCBs can be 3D-printed and taped to the slabs (see FIG. 11 for the mount design).

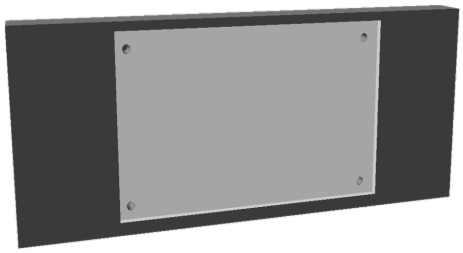

FIG. 11. 3D model of the PCB mount. The PCB will be screwed into the indent in the middle, and the mount will be taped along the edge of a slab.

The addition of the summing amplifier described in this paper will significantly improve the charge sensitivity of the slab detector. milliQan will be up and running for Run 3 of the LHC, expanding the horizons of experimental particle physics in search of millicharged particles.

V. ACKNOWLEDGMENTS

I would like to thank Dr. Sathya Guruswamy, site director for the UCSB Physics REU, for hosting an exceptional summer research experience and ensuring a high quality remote program. This project would not have been possible without my advisor, Dr. David Stuart, whose comprehensive guidance and support was invaluable this summer. Thank you to Ryan Schmitz, my graduate student mentor, for teaching me the physics of millicharged particles and always being willing to help me out at a moment's notice. I would also like to acknowledge all of the collaborators on the milliQan experiment. Finally, thank you to the National Science Foundation for funding this work, which was supported by the NSF REU grant PHY-1852574.

Appendix A: Schematics

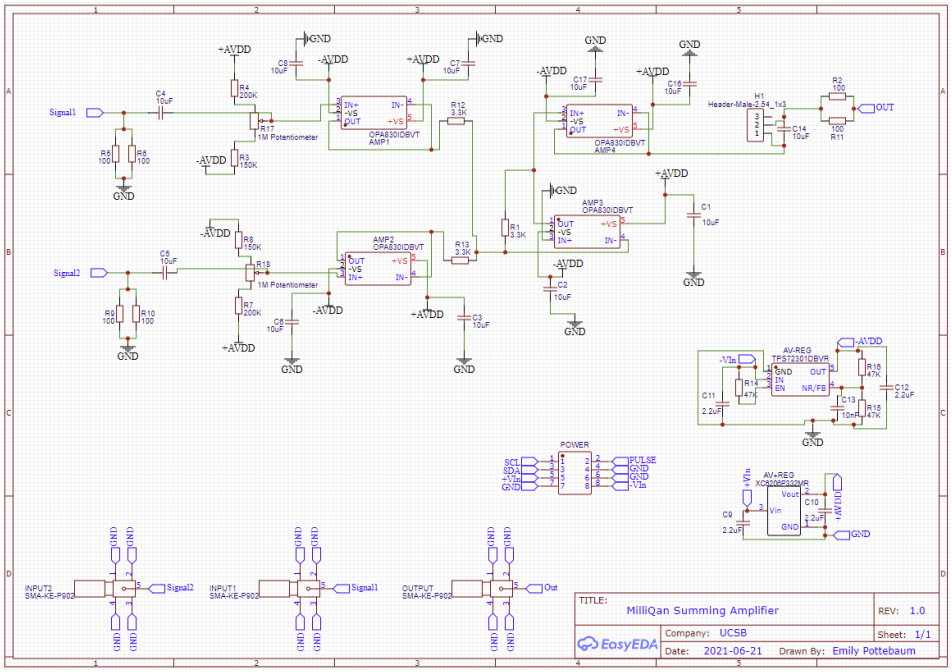

FIG. 12. Schematic for the original summing amplifier design.

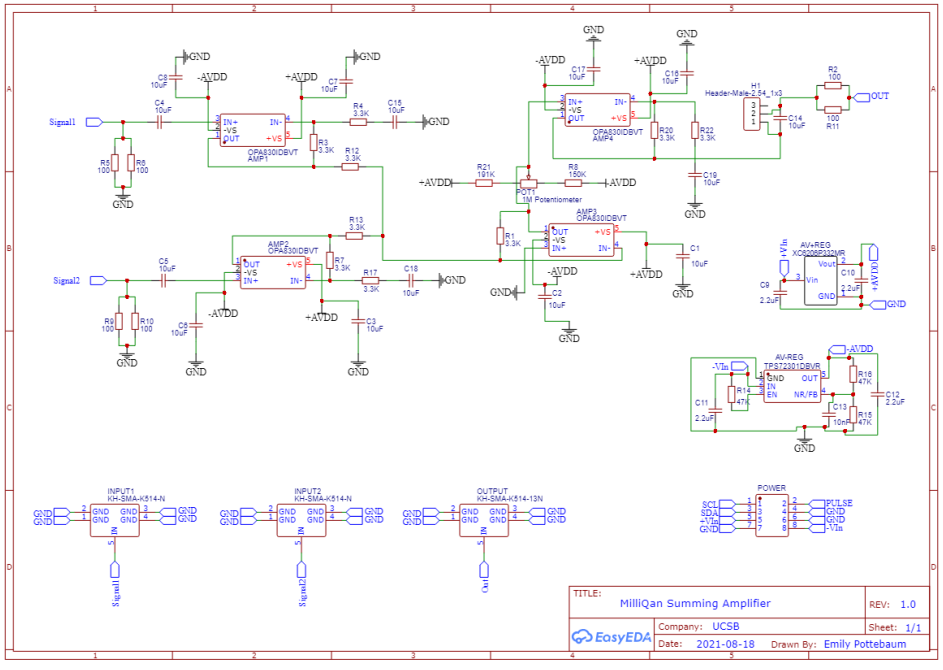

FIG. 13. Schematic for the final summing amplifier design.

[1] O. Buchmueller, C. Doglioni, and L.-T. Wang. Search for dark matter at colliders. *Nature Phys* **13**, 217-223 (2017). https://doi.org/10.1038/nphys4053

[2] M. Fabbrichesi, E. Gabrielli, and G. Lanfranchi. The dark photon. *SpringerBriefs in Physics* 5-8 (2020). https://doi.org/10.1007/978-3-030-62519-1

[3] N. Vinyoles and H. Vogel. Minicharged particles from the Sun: a cutting-edge bound. *JCAP* **03** 002 (2016). https://doi.org/10.1088/1475-7516/2016/03/002

[4] A. Ball et al. Sensitivity to millicharged particles in future proton-proton collision at the LHC. (2021). arXiv:2104.07151

[5] M. Dittrich. Catching cosmic rays. (2020). https://reu.physics.ucsb.edu/past